

## Optimum protocol for fast-switching free-energy calculations

Philipp Geiger and Christoph Dellago\*

*Faculty of Physics, University of Vienna, Boltzmannngasse 5, 1090 Vienna, Austria*

(Received 1 November 2009; published 23 February 2010)

Free-energy differences computed from fast-switching simulations or measurements according to the Jarzynski equation are independent of the particular protocol specifying how the control parameter is changed in time. In contrast, the average work carried out on the system as well the accuracy of the resulting free energy strongly depend on the protocol. Recently, Schmiedl and Seifert [Phys. Rev. Lett. **98**, 108301 (2007)] found that protocols that minimize the average work for a given duration of the switching process have discrete steps at the beginning and the end. Here we determine numerically the protocols that minimize the statistical error in the free energy estimate and find that such minimum error protocols have similar discrete jumps. Our analysis shows that the reduction in computational effort achieved by the use of steplike protocols can be considerable. Such large savings of computing time, however, typically occur for parameter ranges in which an application of the Jarzynski equation is impractical due to large statistical errors arising from the exponential work average.

DOI: [10.1103/PhysRevE.81.021127](https://doi.org/10.1103/PhysRevE.81.021127)

PACS number(s): 05.70.Ln, 05.10.-a

### I. INTRODUCTION

According to the Clausius inequality, a corollary of the second law of thermodynamics, the work  $W$  carried out on a macroscopic system in contact with a heat bath by manipulating a control parameter exceeds the free-energy difference  $\Delta F$  between the equilibrium states corresponding to the initial and final value of the control parameter,

$$W \geq \Delta F. \quad (1)$$

The equal sign in this relation holds if the process is carried out reversibly and the system is in equilibrium at all times during the transformation. If the nonequilibrium transformation is carried out on a microscopic system, for instance a strand of RNA stretched with optical tweezers, the values of the work performed during different realizations of the process differ due to thermal fluctuations leading to a statistical work distribution  $p(W)$ . In this case, individual work values typically exceed the free-energy difference  $\Delta F$  but, occasionally, they can be smaller than  $\Delta F$ , seemingly violating the Clausius inequality and, hence, the second law of thermodynamics. In the average over many realizations of the nonequilibrium process, however, Eq. (1) remains valid as required from fundamental thermodynamics.

Based on the Clausius inequality, one can estimate free-energy differences in experiments and simulations by measuring the work carried out in slow transformations, with corrections derived from fluctuation-dissipation relations that take into account small deviations from equilibrium [1]. It became clear in the past decade or so, however, that fluctuations of nonequilibrium work carry important information about the equilibrium properties of the system that goes far beyond that obtainable from linear response theory. Most notably, the Clausius inequality can be turned into an equality by averaging over the work exponential rather than the work itself [2],

$$e^{-\beta\Delta F} = \langle e^{-\beta W} \rangle. \quad (2)$$

Here, the angular brackets  $\langle \dots \rangle$  indicate an average over many realizations of the nonequilibrium process starting from initial conditions distributed according to the Boltzmann-Gibbs distribution at reciprocal temperature  $\beta = 1/k_B T$ . This exact equation, now known as the Jarzynski nonequilibrium work theorem, relates the equilibrium free-energy difference  $\Delta F$  to the statistics of nonequilibrium work  $W$ . Remarkably, this relation holds under very general conditions [3,4] regardless of how strongly the system is driven away from equilibrium. In other words, the Jarzynski theorem is valid for an arbitrary protocol  $\lambda(t)$  according to which the control parameter  $\lambda$  is switched from its initial value  $\lambda_i$  to its final values  $\lambda_f$  in finite time  $\tau$ . A related result is the Crooks fluctuation theorem, which connects the work distributions of the forward process and the reverse process, in which the control parameter is varied according to the time-reversed forward protocol [5,6].

The nonequilibrium work theorem offers an interesting way of computing free-energy differences from simulations [2] or experiments [8,7]. In both cases, the procedure suggested by Eq. (2) is essentially the same. One first equilibrates the system at reciprocal temperature  $\beta$  with the control parameter fixed at its initial value  $\lambda_A$ . Then, one changes  $\lambda$  from  $\lambda_A$  to  $\lambda_B$  following a given protocol  $\lambda(t)$ . During the transformation, the system evolves in time according to the underlying dynamics and a certain amount of work is performed on the system via the change in the control parameter. Repeating this procedure many times with different initial conditions and averaging the work exponential  $\exp(-\beta W)$  over the work values obtained in the individual realizations of the nonequilibrium process one obtains an estimate for the free-energy difference  $\Delta F$ .

The accuracy of the free-energy estimate computed following this algorithm strongly depends on the protocol used for changing the control parameter [8–10]. As in conventional methods for free-energy computations, the accuracy of the calculation crucially depends on the ability of the proce-

\*christoph.dellago@univie.ac.at

ture to sample all important parts of configuration/phase space [11]. For slow switching, the system is capable of exploring all relevant phase space regions and the work distribution  $P(W)$  is strongly peaked around the free-energy difference  $\Delta F$ . In this case, the exponential work average converges rapidly leading to an accurate free-energy estimation. However, slow switching trajectories are long and therefore computationally costly. Therefore, one would in general prefer to perform the work process at a higher switching rate using shorter trajectories and driving the system strongly out of equilibrium. The resulting work distribution is then typically shifted to larger work values and the exponential average of Eq. (2) is dominated by rare work values leading to slow convergence of the exponential work average [9,10,12]. The statistical errors arising in this case can easily offset the computational benefit of short trajectories [9] such that fast-switching method based on the non-equilibrium work theorem are, in general, not superior to conventional free-energy calculation methods such as Zwanzig's thermodynamics perturbation approach [13] or Kirkwood's thermodynamic integration method [14].

While the rate at which the nonequilibrium process is carried out is certainly the most important parameter determining the statistical error in the free-energy estimate, also the particular shape of the protocol for a given total switching time  $\tau$  can play a significant role. From a computational perspective it is useful to determine the protocol that minimizes the numerical cost of obtaining a certain accuracy in the free-energy estimate. Recently, Schmiedl and Seifert have addressed this question and have determined the protocol that yields the smallest average work for driven systems evolving according to overdamped stochastic dynamics [15]. Analyzing two different one-dimensional models, a colloidal particle dragged in a moving laser trap and a colloidal particle in a harmonic trap with changing strength, Schmiedl and Seifert found that the optimum protocol has discontinuous jumps both at the start and the end of the process. This surprising result is in contrast to expectations raised by a linear response analysis, which yielded a smooth optimum protocol free of jumps [16]. For the particle in the moving trap, the protocol with steps leads to a reduction in the average work of up to 12% compared to the linear continuous protocol. Subsequently, Then and Engel [17] have studied numerically a nonlinear system for different parameters and have found that the system can have one, two, or even more jumps and that there is not only one optimal protocol, but a family of them. More recently, Gomez-Martin, Schmiedl, and Seifert [18] have determined the optimum protocol for underdamped rather than overdamped stochastic dynamics. Also for this type of dynamics the steps in the protocol persist and, moreover, they are complemented by delta-like singularities occurring at the start and at the end of the switching process.

While protocols with steps were shown to minimize the average work carried out during the switching process, the accuracy of the free-energy estimate, however, is not directly related to the average work and a protocol optimized with respect to the average work does not necessarily minimize the statistical error in the free energy [10,12]. Rather, the statistical error depends on the variance of the work expo-

nenial. In the present paper we determine numerically protocols that minimize the statistical error and compare them to protocols that minimize the average work. In particular, we address the question of whether the discontinuous steps found at the beginning and end of the minimum work protocol will also appear for the minimum error protocol. We find that for the cases studied here, the two protocols are similar. In particular, steplike discontinuities of similar magnitude appear also when optimizing the accuracy of the free-energy estimate.

The remainder of this paper is organized as follows. In Sec. II we specify the fast-switching procedure in detail and explain how the statistical errors in the free energy can be estimated. In Sec. III we present the numerical procedure we use for the protocol optimization. This method is then applied in Sec. IV to various fast-switching processes. Some conclusions are provided in Sec. V.

## II. ERROR ESTIMATION

Several methods based on the Jarzynski nonequilibrium work theorem and the Crooks fluctuation theorem have been developed recently for the extraction of free energies from fast-switching measurements of simulations [8,19–30,32]. Here, we will focus our analysis on the protocol optimization for the straightforward application of the Jarzynski equation.

To set the notation, consider a system with energy  $H(x, \lambda)$  depending on the system state  $x$  consisting of the particle positions and, if necessary, the particle momenta, and the control parameter  $\lambda$ . The free-energy difference between the two equilibrium states  $A$  and  $B$  corresponding to  $\lambda_A$  and  $\lambda_B$ , respectively, is then given by

$$\Delta F = F_B - F_A = -k_B T \ln \frac{\int dx \exp\{-\beta H(x, \lambda_B)\}}{\int dx \exp\{-\beta H(x, \lambda_A)\}}. \quad (3)$$

As the control parameter is switched in time  $\tau$  from its initial to its final value following the protocol  $\lambda(t)$ , the work

$$W[x(t), \lambda(t)] = \int_0^\tau dt \dot{\lambda} \frac{\partial}{\partial \lambda} H[t, \lambda(t)] \quad (4)$$

is performed on the system. In the above equation, the notation  $W[x(t), \lambda(t)]$  indicates that the work depends both on protocol  $\lambda(t)$  as well as on the particular trajectory  $x(t)$  followed by the system. By generating  $N$  trajectories starting from initial conditions distributed according to  $\rho(x) \propto \exp\{-\beta H(x, \lambda_A)\}$ , one obtains the free-energy estimate

$$\Delta \bar{F}_N = -k_B T \ln \frac{1}{N} \sum_{i=1}^N \exp(-\beta W^{(i)}), \quad (5)$$

where  $W^{(i)}$  denotes the work performed along the  $i$ th trajectory. Due to the nonlinearity of the logarithm, this free-energy estimator is biased, i.e., the expectation value of  $\Delta \bar{F}_N$  differs from the free-energy difference  $\Delta F$ . In addition to the bias, the free-energy estimator from Eq. (5) is affected by statistical errors. In the large sample limit, i.e., for large  $N$ , the bias can be neglected compared to the statistical error and, for statistically independent work values, the mean

squared deviation of the free-energy estimator  $\Delta\bar{F}_N$  from  $\Delta F$  is given by [8,31]

$$\varepsilon^2 \equiv \langle (\Delta\bar{F}_N - \Delta F)^2 \rangle = \frac{k_B^2 T^2}{N} \{ \langle \exp(-2\beta W_{\text{diss}}) \rangle - 1 \}, \quad (6)$$

where the dissipative work  $W_{\text{diss}}$  is defined as the work performed in excess of the free-energy difference  $\Delta F$ ,

$$W_{\text{diss}} \equiv W - \Delta F. \quad (7)$$

Thus, the expectation value of the error essentially depends on  $\langle \exp(-2\beta W) \rangle$  and it is this quantity one has to minimize with respect to the protocol  $\lambda(t)$  in order to optimize the accuracy of the free-energy calculation. Note that the average  $\langle \exp(-2\beta W) \rangle$  is fully determined by  $P(W)$ , the distribution of work carried out during the switching process.

Numerical procedures to minimize the statistical error in the free energy, such as the one discussed in the next section, rely on an accurate determination of the average  $\langle \exp(-2\beta W) \rangle$  as well as its gradient with respect to the protocol  $\lambda(t)$ . The estimator of this average, however, is typically affected by statistical uncertainties that due to the squared exponential by far exceed those of the exponential average  $\langle \exp(-\beta W) \rangle$  evaluated in applications of the Jarzynski equation. Since statistical errors often even make a direct calculation of Jarzynski's exponential work average impractical, an accurate error estimation based on the numerical calculation of the average  $\langle \exp(-2\beta W) \rangle$  seems exceedingly demanding.

This computational difficulty can be alleviated by expressing the average  $\langle \exp(-2\beta W) \rangle$  in terms of the work performed on the system during the reverse process. Using the Crooks fluctuation theorem, one can show that [12]

$$\langle \exp(-2\beta W) \rangle = \exp(-\beta \Delta F) \langle \exp(\beta W) \rangle_R, \quad (8)$$

where the notation  $\langle \dots \rangle_R$  indicates an average over realizations of the reverse process. As a result, minimizing  $\langle \exp(-2\beta W) \rangle$  with respect to the forward protocol is mathematically equivalent to minimizing the average  $\langle \exp(\beta W) \rangle_R$  for the time reversed protocol  $\lambda_R(t) = \lambda(\tau - t)$ . Depending on the work distribution  $P(W)$ , the fluctuations of  $\exp(\beta W)$  can be much more benign than those of  $\exp(-2\beta W)$  leading to major savings in the estimation of the statistical error in the free energy. Using Eq. (8), the expected error can be expressed in terms of the dissipative work  $W_{\text{diss}}^R = W + \Delta F$  carried out during the reverse process [12],

$$\varepsilon^2 = \frac{k_B^2 T^2}{N} \{ \langle \exp(\beta W_{\text{diss}}^R) \rangle_R - 1 \}. \quad (9)$$

It follows [12] that about

$$N_{kT} = \langle \exp(-2\beta W) \rangle = \langle \exp(\beta W_{\text{diss}}^R) \rangle_R \quad (10)$$

trajectories are required to obtain an accuracy of  $k_B T$  in the estimation of the free energy, a result derived previously by Jarzynski following a different route [10]. Thus, the protocol that optimizes the accuracy (or, equivalently, minimizes the number of trajectories required to obtain a given error level) in forward direction, minimizes the exponential average of the dissipative work carried out in the reverse process.

The extent with which the error estimation based on the time-reversed process can facilitate the estimation of error can be illustrated using a simple model consisting of a particle dragged by a moving harmonic trap under the influence of friction and noise (see Sec. IV A). For a trap translated at constant velocity  $v$ , the work distribution is Gaussian,

$$P(W) = \frac{1}{\sqrt{2\pi\sigma_W^2}} \exp\left\{ -\frac{(W - \langle W \rangle)^2}{2\sigma_W^2} \right\}, \quad (11)$$

with average  $\langle W \rangle$  and variance  $\sigma_W^2$  depending on the temperature, the friction constant, the force constant and velocity of the trap, and the translated distance [12]. In this case, average work and variance are related by  $2\langle W \rangle = \beta\sigma_W^2$  and the forward and backward process are identical such that we can drop the subscript  $R$ .

For this simple model, the expected errors for the averages  $\langle \exp(-2\beta W) \rangle$  and  $\langle \exp(\beta W) \rangle$  can be calculated analytically,

$$\varepsilon_{\text{fw}}^2 = \frac{1}{N} \langle [\delta e^{-2\beta W}]^2 \rangle = \frac{1}{N} [e^{12\beta\langle W \rangle} - e^{4\beta\langle W \rangle}], \quad (12)$$

$$\varepsilon_{\text{bw}}^2 = \frac{1}{N} \langle [\delta e^{\beta W}]^2 \rangle = \frac{1}{N} [e^{6\beta\langle W \rangle} - e^{4\beta\langle W \rangle}]. \quad (13)$$

Here, the notation  $\delta A = A - \langle A \rangle$  denotes the deviation of a quantity from its average. According to the above equations, if  $N_{\text{fw}}$  forward trajectories are required to obtain a certain accuracy of the error estimator, the same accuracy can be obtained from  $N_{\text{bw}} \approx \sqrt{N_{\text{fw}}}$  backward trajectories. The statistical error of the exponential average appearing in the Jarzynski equation is given by

$$\frac{1}{N} \langle [\delta e^{-\beta W}]^2 \rangle = \frac{1}{N} [e^{2\beta\langle W \rangle} - 1] \quad (14)$$

such that even less trajectories are required to obtain the same accuracy in the estimation of this average.

In summary, the results obtained above for a simple model which can be solved analytically indicate that the computational cost of estimating errors in the free energy can be reduced considerably by determining it from trajectories computed for the backward rather than the forward transformation. After the optimization has been performed by minimizing  $\langle \exp(\beta W) \rangle$  for the backward process, the optimum protocol of the forward process is obtained from that of the backward process by simple time inversion,  $\lambda(t) = \lambda_R(\tau - t)$ .

### III. NUMERICAL PROTOCOL OPTIMIZATION

Previous efforts to find optimum protocols were directed toward the minimization of the average work performed during the switching process [15–18,33]. Here, instead, we determine the protocol that optimizes the accuracy of the free-energy calculation. As discussed in the previous section, the statistical error in the free-energy estimator is not simply related to the average work, such that these two optimization approaches may yield different results. While the minimum work protocol can be determined analytically for simple sys-

tems using a variational approach [15], this is no longer possible for the minimum error protocol. We therefore resort to a numerical optimization scheme introduced in this section.

To solve the optimization problem it is first necessary to define a sufficiently general function space for the switching protocol. One possibility, which we will use in Sec. IV, consists in discretizing the protocol and specifying it at evenly spaced time steps. In this case, the discrete values of the control parameter are the parameters with respect to which the optimization is carried out. In the following we let  $\alpha$  denote this set of optimization parameters. A less general function space for the protocol  $\lambda(t)$  comprises smooth polynomials complemented with discrete steps at the beginning and the end. In this case, the coefficients of the polynomial are the relevant optimization parameters and the optimization space is typically much lower dimensional. However, such a choice provides less freedom and precludes the formation of steps at positions other than the beginning and the end.

To find the optimum protocol we need to minimize the figure of merit, the average work or the expected statistical error, with respect to the parameters. While various optimization methods can be used for this purpose [34], algorithms guided by the gradient of the target function are, in general, more efficient than others. In our case, the target function is an ensemble average over nonequilibrium trajectories and its gradient can be determined in the following way. Consider a general quantity (functional)  $A[x(t), \alpha]$  depending on the trajectory  $x(t)$  and the protocol  $\lambda(t)$  represented by the set of parameters  $\alpha$ . The average of  $A$  in the ensemble of nonequilibrium pathways can be written as

$$\langle A(\alpha) \rangle = \int \mathcal{D}x(t) \mathcal{P}[x(t), \alpha] A[x(t), \alpha], \quad (15)$$

where  $\int \mathcal{D}x(t)$  denotes the integration over all pathways and  $\mathcal{P}[x(t), \alpha]$  is the probability of pathway  $x(t)$  given the protocol parameters  $\alpha$ . The gradient of this average with respect to the protocol parameters  $\alpha$  is then obtained by differentiating the integrand,

$$\begin{aligned} \nabla_{\alpha} \langle A(\alpha) \rangle &= \int \mathcal{D}x(t) [(\nabla_{\alpha} \mathcal{P})A + \mathcal{P} \cdot \nabla_{\alpha} A] \\ &= \int \mathcal{D}x(t) [(\mathcal{P} \nabla_{\alpha} \ln \mathcal{P})A + \mathcal{P} \cdot \nabla_{\alpha} A] \\ &= \langle (\nabla_{\alpha} \ln \mathcal{P})A \rangle + \langle \nabla_{\alpha} A \rangle. \end{aligned} \quad (16)$$

In going from the first to the second line of the above equation, we have used the identity  $\nabla_{\alpha} \mathcal{P} = \mathcal{P} \nabla_{\alpha} \ln \mathcal{P}$  so that we can write both terms of the right-hand side as path averages.

For the averages  $\langle W \rangle$ ,  $\langle \exp(-2\beta W) \rangle$ , and  $\langle \exp(\beta W) \rangle$  the gradients with respect to the optimization parameters are

$$\nabla_{\alpha} \langle W(\alpha) \rangle = \langle (\nabla_{\alpha} \ln \mathcal{P})W \rangle + \langle \nabla_{\alpha} W \rangle, \quad (17)$$

$$\nabla_{\alpha} \langle e^{-2\beta W} \rangle = \langle (\nabla_{\alpha} \ln \mathcal{P})e^{-2\beta W} \rangle - 2\beta \langle (\nabla_{\alpha} W)e^{-2\beta W} \rangle, \quad (18)$$

and

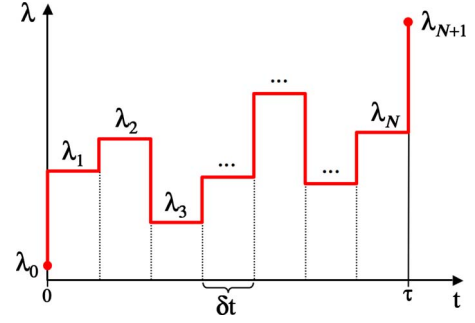


FIG. 1. (Color online) Steplike protocol  $\lambda(t)$  used in all calculations. The protocol is optimized with respect to the control parameter values  $\{\lambda_1, \lambda_2, \dots, \lambda_{N-1}, \lambda_N\}$  for fixed  $\lambda_i = \lambda_0$  and  $\lambda_f = \lambda_{N+1}$ .

$$\nabla_{\alpha} \langle e^{\beta W} \rangle = \langle (\nabla_{\alpha} \ln \mathcal{P})e^{\beta W} \rangle + \beta \langle (\nabla_{\alpha} W)e^{\beta W} \rangle, \quad (19)$$

respectively. Thus, for a particular parameter set  $\alpha$ , these gradients can be computed as averages over nonequilibrium pathways determined with the corresponding protocol. One can then minimize the target function using a steepest descent or conjugate gradient procedure [34], in which new gradients are determined after each step in parameter space. The iteration is stopped when a local minimum is reached as detected by the magnitude of the gradient falling below a certain threshold.

In numerical simulations, the time evolution of the system is usually followed in small time steps  $\delta t$  and trajectories are represented by discrete sets of points,  $x(t) = \{x_0, x_1, x_2, \dots, x_{N-1}, x_N\}$ , where configuration  $x_i$  is reached after  $i$  time steps. In this case, also the protocol  $\lambda(t)$  needs to be appropriately discretized. Here, we approximate the protocol by a piecewise constant function that takes the values  $\lambda_j$  in the time interval  $(j-1)\delta t < t < j\delta t$  as shown schematically in Fig. 1. The dynamics is then carried out in the following way. For a given initial condition  $x_0$ , first the control parameter is changed from its initial value  $\lambda_0 = \lambda_i$  to  $\lambda_1$ . Then a dynamical step is performed for a control parameter fixed at  $\lambda_1$  carrying the system from  $x_0$  to  $x_1$ . Next, the control parameter is changed from  $\lambda_1$  to the value  $\lambda_2$  at fixed system configuration  $x_1$ , after which the control parameter is changed from  $\lambda_2$  to  $\lambda_3$ . This sequence of operations is then repeated until the system reaches configuration  $x_N$  after a total of  $N$  steps. As a final operation, the control parameter is changed from  $\lambda_N$  to its final values  $\lambda_{N+1} = \lambda_f$ . This final step is done for symmetry such that also the reverse process starts with a change in the control parameter. Thus, the discretized version of the protocol is given by  $\lambda(t) = \{\lambda_0, \lambda_1, \lambda_2, \dots, \lambda_N, \lambda_{N+1}\}$ . Schematically, the dynamics of the system under the changing control parameter can be represented as

$$\lambda_0 \rightarrow \lambda_1, \quad x_0 \rightarrow x_1, \quad \dots, \quad x_{N-1} \rightarrow x_N, \quad \lambda_N \rightarrow \lambda_{N+1}. \quad (20)$$

Here, the symbol over the arrow indicates the quantity held fixed while the corresponding step happens either by direct manipulation,  $\lambda_j \rightarrow \lambda_{j+1}$ , or following the dynamics of the system,  $x_j \rightarrow x_{j+1}$ . Since  $\lambda_0 = \lambda_i$  and  $\lambda_{N+1} = \lambda_f$ , the initial and final values of the control parameter, are given, only the

intervening values can be tuned to minimize the average work or the expected statistical error. Thus, in this case, the parameter set  $\alpha$  that controls the shape of the protocol is given by the  $N$  values of the control parameter,  $\alpha = \{\lambda_1, \lambda_2, \dots, \lambda_{N-1}, \lambda_N\}$ .

In computing the derivatives  $\nabla_\alpha \ln \mathcal{P}$  and  $\nabla_\alpha W$  with respect to the control parameter values  $\lambda_j$  it is necessary to take into account the conventions for the switching process specified in the previous paragraph. In particular, work is carried out only during the changes of the control parameter leading to the total work

$$W = \sum_{i=0}^N H(x_i, \lambda_{i+1}) - H(x_i, \lambda_i) \quad (21)$$

performed along a particular trajectory  $x(t)$ . From this expression it is straightforward to calculate the derivatives  $\partial W / \partial \lambda_j$  for a specific energy function  $H(x, \lambda)$ . Similar derivatives need to be taken in the calculation of  $\partial \ln \mathcal{P} / \partial \lambda_j$ . For the stochastic dynamics considered in the next section this poses no difficulties.

#### IV. EXAMPLE APPLICATIONS

In this section we determine optimum protocols for a few simple models ranging from a particle in a harmonic trap, for which the protocol has been optimized analytically by Schmiedl and Seifert [15], to a polymer whose end points are separated from each other by an external force.

##### A. Shifted harmonic trap

Consider a colloidal particle moving in one-dimension through a viscous liquid with a harmonic laser trap. The motion of the trap is specified by the control parameter  $\lambda(t)$ , the center of the trap, which is changed from its initial value  $\lambda_i$  at time  $t=0$  to its final value  $\lambda_f$  at time  $\tau$ . During the translation the trap is felt by the particle as a quadratic external potential with force constant  $k$ ,

$$U(x, t) = \frac{k}{2} [x - \lambda(t)]^2, \quad (22)$$

where  $x$  denotes the position of the particle. For sufficiently large friction, the motion of the particle can be described by an overdamped Langevin equation,

$$\gamma \dot{x} = f + \xi, \quad (23)$$

where  $\gamma$  is the friction coefficient and  $f = -k[x - \lambda(t)]$  is the external force. The random force  $\xi$  is modeled as  $\delta$ -correlated Gaussian white noise with vanishing mean,  $\langle \xi(t) \rangle = 0$ , and a variance given by the fluctuation-dissipation theorem,  $\langle \xi(t) \xi(t') \rangle = 2\gamma k_B T \delta(t - t')$ . The diffusion constant  $D$  is related to the friction coefficient by the Einstein relation  $D = k_B T / \gamma$ . Note that for this model, the free energy does not depend on the trap position and therefore the free energy between the equilibrium states corresponding to the initial and final position of the laser trap vanishes,  $\Delta F = 0$ . Also, the forward and backward processes are identical and lead to the same work distribution.

The stochastic equation of motion (23) can be integrated in small time steps  $\delta t$  under the assumption that the force  $f(x)$  is constant during the time step [35],

$$x_{(i+1)\delta t} = x_{i\delta t} + \beta D \delta t f(x_{i\delta t}) + \delta x, \quad (24)$$

where  $\delta x$  is a random variable drawn from a Gaussian distribution with zero average and a variance of  $2D\delta t$ . Since overdamped Langevin dynamics is Markovian, the probability of a particular discretized trajectory  $x(t) = \{x_0, x_{\delta t}, x_{2\delta t}, \dots, x_\tau\}$  with time step  $\delta t$  can be written as a concatenation of short time transition probabilities,

$$\mathcal{P} = \frac{e^{-\beta U(x_0, \lambda_i)}}{Z(\lambda_i)} \prod_i p[x_{i\delta t} \rightarrow x_{(i+1)\delta t}], \quad (25)$$

where  $Z(\lambda_i)$  is the partition function corresponding to the initial value of the control parameter. For overdamped Langevin dynamics, the short time transition probability  $p(x \rightarrow y)$  is given by [36]

$$p(x \rightarrow y) = \frac{1}{\sqrt{4\pi D \delta t}} \exp\left\{-\frac{(y - x - \beta D \delta t f)^2}{4D \delta t}\right\}. \quad (26)$$

where  $f = -k[x - \lambda(t)]$  is the force exerted on the particle by the moving trap. Since the external force depends on the trap position, the path probability is a functional of the protocol  $\lambda(t)$ .

For this model, Schmiedl and Seifert determined, using a variational approach, the protocol  $\lambda^*(t)$  that minimizes the average work carried out for given initial and trap final positions,  $\lambda_i = 0$  and  $\lambda_f$ , and a total time  $\tau$  [15],

$$\lambda^*(t) = \begin{cases} 0 & \text{for } t = 0, \\ \lambda_f \frac{\kappa t + 1}{\kappa \tau + 2} & \text{for } 0 < t < \tau, \\ \lambda_f & \text{for } t = \tau. \end{cases} \quad (27)$$

where  $\kappa \equiv k / \gamma$  is a constant with unit of one over time. The inverse of  $\kappa$  is the typical relaxation time of the system in the trap with force constant  $k$ . Thus, this optimum work protocol has two discrete jumps of equal size

$$\Delta \lambda = \frac{\lambda_f}{\kappa \tau + 2} \quad (28)$$

at the beginning and at the end. Between the jumps, the protocol is linear with slope  $\lambda_f \kappa / (\kappa \tau + 2)$ . Thus, the jumps are largest for instantaneous switching,  $\tau = 0$ , and they vanish in the slow switching limit,  $\tau \rightarrow \infty$ .

The average work carried out for the optimum protocol,

$$\langle W \rangle^* = \frac{k \lambda_f^2}{\kappa \tau + 2}, \quad (29)$$

is smaller than that of the linear process,

$$\langle W \rangle^{\text{lin}} = k \lambda_f^2 \frac{\kappa \tau + e^{-\kappa \tau} - 1}{\kappa^2 \tau^2}, \quad (30)$$

by as much as 14% for  $\tau = 2.69 \kappa^{-1}$  [15]. Note that the work ratio  $\langle W \rangle^* / \langle W \rangle^{\text{lin}}$  does not depend on the trap displacement  $\lambda_f$  but only on the total time of the switching process. The

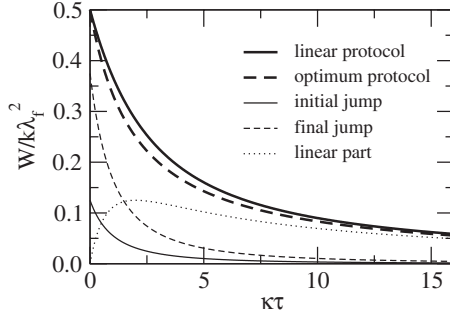


FIG. 2. Average work as a function of the switching time  $\tau$  for the linear protocol (thick solid line) and the optimum protocol (thick dashed line). Also shown are the average work contributions of the initial jump (thin solid line), the final jump (thin dashed line) and the linear part (thin dotted line) of the optimum protocol.

average work carried out for the linear and the optimum protocol is shown in Fig. 2 as a function of the switching time  $\tau$ .

Although the jumps at the beginning and the end have equal size, the work carried out during the two jumps differs. The average work for the first jump can be easily calculated as integral over the initial equilibrium distribution,

$$\langle W \rangle_i^* = \frac{k\lambda_f^2}{2(\kappa\tau + 2)^2}. \quad (31)$$

To determine the average work for the jump at the end one needs to know the position distribution of  $\rho(x, \tau)$  at time  $\tau$  just before the final jump. This distribution can be determined explicitly by solving the appropriate Fokker-Planck equation for the trap moving at constant speed between the two jumps [37]. Integration over  $\rho(x, \tau)$  then yields

$$\langle W \rangle_f^* = \frac{3k\lambda_f^2}{2(\kappa\tau + 2)^2}. \quad (32)$$

The work carried out during the uniform translation of the trap between the jumps is given by

$$\langle W \rangle_l^* = \langle W \rangle^* - \langle W \rangle_i^* - \langle W \rangle_f^* = \frac{\kappa\tau k\lambda_f^2}{(\kappa\tau + 2)^2}. \quad (33)$$

Thus, for all switching times, the work carried out during the final step is three times larger than that performed at the start,  $\langle W \rangle_f = 3\langle W \rangle_i$ . While in the limit of short switching times,  $\tau \rightarrow 0$ , all the work is carried out during the two jumps, the linear part of the protocol contributes most to the average work for long switching times,  $\tau \rightarrow \infty$ . The work carried out at the jumps and during the linear part of the protocol is displayed in Fig. 2 as a function of the switching time  $\tau$ .

An interesting question is how the position distribution  $\rho(x, t)$  evolves in time for the optimum protocol. Due to the shape of the trap, the initial distribution  $\rho(x, 0)$  is Gaussian with mean  $\langle x(0) \rangle = \lambda_i$  and variance  $\sigma_x^2(0) = 1/\beta k$ . Since in the Fokker-Planck equation for the parabolic trap the coefficients are independent of the position, a distribution which is Gaussian initially will remain Gaussian for all later times with time-dependent average  $\langle x(t) \rangle$  and variance  $\sigma_x^2(t)$  [37,38]. In general, the particular time evolution of the aver-

age and the variance depend on the shape of the protocol  $\lambda(t)$  [37,38]. Since the initial distribution is the Boltzmann-Gibbs equilibrium distribution, the variance of  $\rho(x, t)$  does not change in time,  $\sigma_x^2(t) = 1/\beta k$ . The time evolution of the center  $\langle x(t) \rangle$  of the distribution is given by [38]

$$\langle x(t) \rangle = \kappa \int_0^t dt' e^{-\kappa(t-t')} \lambda(t'). \quad (34)$$

For the optimum protocol, integration yields

$$\langle x(t) \rangle = \frac{\lambda_f \kappa t}{\kappa\tau + 2}. \quad (35)$$

Thus, in the case of the optimum protocol, the time-dependent distribution  $\rho(x, t)$  is a Gaussian with constant variance moving with the same speed of the trap. The lag between the trap and the center of the distribution is equal to the jump size  $\Delta\lambda$ . Note that such a constant lag arises only for the particular jump size of the optimum protocol. Only then is the distribution in the right position with respect to the trap from the beginning of the switching process. For all other jump sizes (including a vanishing jump size), the lag approaches  $\Delta\lambda$  exponentially with time constant  $\kappa^{-1} = \gamma/k$ . Apparently, the work savings obtained in this particular situation during the linear translation of the trap are sufficient to compensate for the extra work carried out during the discrete jumps at the beginning and the end of the switching process.

As mentioned previously, the average  $\langle \exp(-2\beta W) \rangle$ , which determines the magnitude of the error in the free energy, is fully determined by the work distribution  $P(W)$ . It is therefore of interest to establish the work distribution for the optimum protocol. This can be done by considering the joint probability distribution  $\rho(x, w, t)$ , where  $w$  is the work accumulated along a particular trajectory up to time  $t$  [37]. Since the coefficients in the corresponding Fokker-Planck equation are constant or linear in  $x$  and  $w$  for a parabolic trap, a distribution which is initially Gaussian will remain Gaussian later with moments that are functions of time. The work distribution can then be obtained from  $\rho(x, w, t)$  by integrating out the position variable  $x$ . Thus, the work distribution  $P(W)$  of the complete switching process is Gaussian for any switching protocol  $\lambda(t)$ , including protocols with discrete steps occurring at arbitrary times. Such a work distribution is fully determined by the average work  $\langle W \rangle$ , because the Jarzynski identity implies that for a Gaussian work distribution the variance  $\sigma_W^2$  is related to the average by  $\Delta F = \langle W \rangle - \beta\sigma_W^2/2$ . This result implies that for Gaussian work distributions minimizing the average work are equivalent to minimizing the work variance.

For Gaussian work distributions the average  $\langle \exp(-2\beta W) \rangle$  can be computed analytically,  $\langle \exp(-2\beta W) \rangle = \exp(2\beta \langle W \rangle)$ . It follows that in this particular case minimizing the average work is equivalent to minimizing the error in the free-energy estimate. Hence, the optimum protocol obtained by Schmiedl and Seifert for the particle in the trap [15] [see Eq. (27)] is also optimal in the sense of free-energy computation. Note, however, that this is not a general result, but is limited to situations with Gaussian work distributions.

The error of the free energy obtained with the optimum protocol relative to that of the linear protocol is then given by

$$\frac{\varepsilon^*}{\varepsilon^{\text{lin}}} = \frac{\sqrt{\langle e^{-2\beta W} \rangle^*}}{\sqrt{\langle e^{-2\beta W} \rangle^{\text{lin}}}} = e^{\beta(\langle W \rangle^* - \langle W \rangle^{\text{lin}})}. \quad (36)$$

Since the error ratio  $\varepsilon^*/\varepsilon^{\text{lin}}$  depends on the work difference  $\langle W \rangle^* - \langle W \rangle^{\text{lin}}$  rather than on the work ratio  $\langle W \rangle^*/\langle W \rangle^{\text{lin}}$ , it reaches its minimum at  $\tau = 1.37\kappa^{-1}$  and not at  $\tau = 2.688\kappa^{-1}$  as the work ratio. The time  $\tau$  at which the work difference  $\langle W \rangle^* - \langle W \rangle^{\text{lin}}$  is a minimum does not depend on the trap displacement  $\lambda_f$ . The magnitude of the error ratio, however, decreases with increasing trap displacement  $\lambda_f$ . While for a trap displacement of  $\lambda_f = 1/\sqrt{\beta k}$  the error ratio is  $\varepsilon^*/\varepsilon^{\text{lin}} = 0.96$ , for  $\lambda_f = 10/\sqrt{\beta k}$  the error ratio is as low as  $\varepsilon^*/\varepsilon^{\text{lin}} = 0.028$  implying a considerable reduction in the computational effort required to obtain a given accuracy.

Since the computational cost of a free-energy calculation is proportional to the number of integrated trajectories, a more relevant measure for the efficiency of a protocol is the number  $N_{kT}$  of trajectories required to obtain a statistical error of about  $1 k_B T$  in the free-energy estimate [see Eq. (10)]. The number  $N_{kT}^*$  of trajectories required for the optimum protocol relative to the number  $N_{kT}^{\text{lin}}$  of trajectories required in the linear protocol is given by

$$\eta = \frac{N_{kT}^*}{N_{kT}^{\text{lin}}} = \exp\{2\beta(\langle W \rangle^* - \langle W \rangle^{\text{lin}})\}. \quad (37)$$

For  $\tau = 1.372\kappa$ , at which the difference in work between the minimum and the linear protocol reaches its minimum, the ratio of required trajectories is  $\eta = 0.93$  and  $\eta = 0.16 \times 10^{-4}$  for trap displacements of  $\lambda_f = 1/\sqrt{\beta k}$  and  $\lambda_f = 4/\sqrt{\beta k}$ , respectively. In the latter case, a total of 13 000 is required to reach an accuracy of  $1 k_B T$  in the free-energy estimate using the optimum protocol. An even more substantial reduction in computation cost results for larger trap displacements. For instance, for a trap displacement of  $\lambda_f = 10/\sqrt{\beta k}$  the computational cost is reduced by more than a factor of  $10^3$ . In this case, however, more than  $10^{25}$  trajectories are needed to reach an accuracy of  $1 k_B T$  even using the optimum protocol. The reduction in computational cost as well as the number of required trajectories are shown in Fig. 3 as a function of the trap displacement for  $\tau = 1.372\kappa^{-1}$ . As can be inferred from the figure, depending on the parameters, the optimum protocol can lead to considerable savings in computing time, which can exceed by far the relative reduction in the average work. It is, however, important to realize that one can exploit such large reductions in computational cost only if the total number of trajectories required to reach the desired statistical accuracy is within the available computing capacity. Frequently, however, the number of required trajectories is beyond what can be computationally achieved such that the potentially large savings in computing time with respect to the linear protocol cannot be realized in practice.

Although for the particle in the translated harmonic trap the minimum error protocol is identical to the minimum work protocol known analytically [see Eq. (27)], we next determine the optimum protocol numerically in order to test

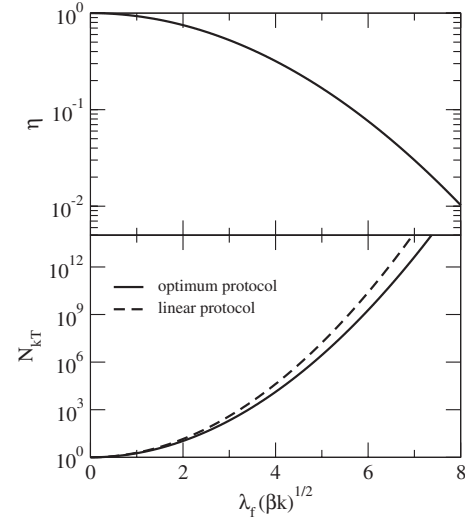


FIG. 3. Top: reduction in computational cost  $\eta = N_{kT}^*/N_{kT}^{\text{lin}}$  as a function of the trap displacement  $\lambda_f\sqrt{\beta k}$  for total time of  $\tau = 1.37\kappa^{-1}$ , at which  $\eta$  is minimal. Bottom: number of trajectories required with the optimum and the linear protocol to obtain an accuracy of  $1 k_B$  as a function of  $\lambda_f\sqrt{\beta k}$  for  $\tau = 1.37\kappa^{-1}$ .

our optimization algorithm. Initial conditions for the fast-switching trajectories are sampled from a Boltzmann distribution. From each initial condition a trajectory of length  $\tau$  is determined by integrating the Langevin equation with the algorithm of Eq. (24). Averaging over all trajectories one obtains the gradients of Eqs. (17)–(19). The gradients are then used in a conjugate gradient algorithm [34] to generate a new set of parameters  $\alpha$ . The size of the conjugate gradient steps is determined empirically rather than by a line minimization. The optimization is terminated as soon as the magnitude of the respective gradient falls below a given threshold.

The results of the protocol optimization, obtained from  $5 \times 10^8$  trajectories of length  $\tau = 1.0\kappa^{-1}$  for the switching from  $\lambda_i = 0$  to  $\lambda_f = 1/\sqrt{\beta k}$  with time step size  $\delta t = 0.002\kappa^{-1}$ , are shown in Fig. 4. Here, the optimization is done in a 500-dimensional parameter space. The protocols determined by minimizing  $\langle W \rangle$  agree very well with the analytical result of Schmiedl and Seifert [15]. As expected, statistically indistinguishable results are obtained if the expected error is minimized instead of the average work.

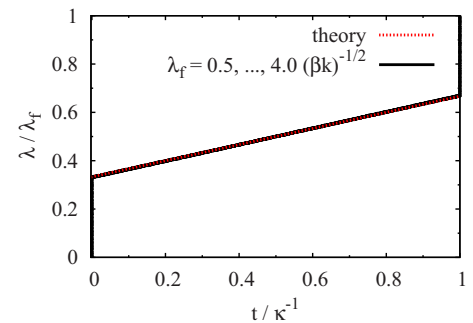


FIG. 4. (Color online) Optimum protocols for the shifted harmonic potential, obtained by minimizing  $\langle W \rangle$  for  $\tau = 1.0\kappa^{-1}$  and different trap displacements ranging from  $\lambda_f = 0.5/\sqrt{\beta k}$  to  $\lambda_f = 4.0/\sqrt{\beta k}$  (solid lines). The dotted line indicates the optimum protocol found analytically by Schmiedl and Seifert [15].

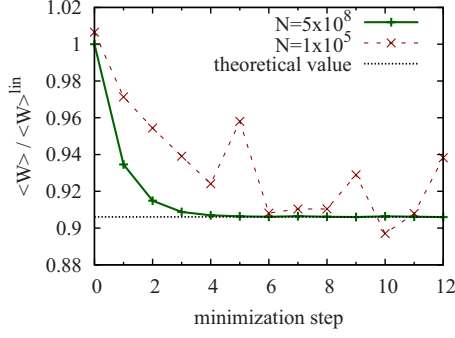


FIG. 5. (Color online) Average work  $\langle W \rangle$  normalized by the average work  $\langle W \rangle^{\text{lin}}$  of the linear protocol as a function of the number of minimization steps determined for  $\tau=1.0\kappa^{-1}$ , a trap displacements of  $\lambda_f=1.0/\sqrt{\beta k}$  and different number of trajectories  $N$  per iteration. The minimization is carried out using a conjugate gradient procedure.

The convergence of the average work to its minimum value in the minimization process is depicted in Fig. 5. After just a few iterations, the average work reaches its minimum, which exactly corresponds to the theoretical result of Schmiedl and Seifert [15]. Note that at least about  $N=100\,000$  trajectories per iteration are required to make the protocol optimization possible. Only then is the statistical error in the average work significantly smaller than the reduction in the average work achievable in the optimization.

### B. V-shaped trap

To study the effects of a nonharmonic trap we determined the optimum protocol also for the V-shaped trap potential

$$U[x, \lambda(t)] = h|x - \lambda(t)|, \quad (38)$$

which exerts a force of constant magnitude  $h$  on the particle driving it toward the trap center. The particle evolves in time according to the overdamped Langevin equation, Eq. (23). As in the case of the harmonic potential, the trap is displaced from  $\lambda_i$  to  $\lambda_f$  in the time  $\tau$  and the free energy does not depend on the trap position  $\lambda$ ,  $\Delta F=0$ . For this particular trap shape the calculation of the gradients of the work and the expected error requires some care, because the kink at  $\lambda=0$  leads to a singularity in the force derivative. Using the appropriate expressions, however, the gradients can be determined numerically without difficulties. In all our numerical calculations we measure energies in units of  $k_B T$ , lengths in units of  $1/(\beta h)$  and times in units of  $\kappa^{-1} = \gamma k_B T / h^2$  corresponding to the choice  $k_B T=1$ ,  $h=1$  and  $\gamma=1$ .

The protocols obtained by minimizing the average work and the expected error are shown in Fig. 6. In each iteration of the optimization procedure  $10^8$  trajectories of length  $\tau=1\kappa^{-1}$  were integrated with time step  $\delta t=0.002\kappa^{-1}$  for a trap displaced from  $\lambda_i=0$  to  $\lambda_f=1/(\beta h)$ . A total of 30–90 iterations were carried out in this 500-dimensional parameter space. As in the case of the harmonic trap, both optimum protocols are characterized by discrete step at the beginning and the end of the switching process. In contrast to the harmonic case, however, the work distributions are strongly

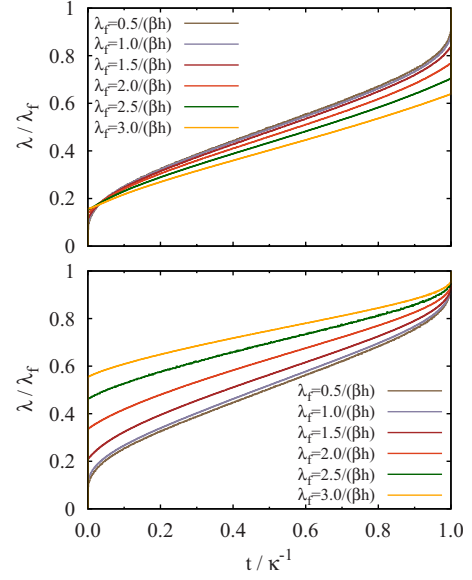


FIG. 6. (Color online) Minimum work protocols (top) and minimum error protocols (bottom) for the V-shaped trap for various trap displacements. The trajectories length was  $\tau=1\kappa^{-1}$ .

non-Gaussian such that the work minimization and the error minimization yield distinctly different protocols.

The work ratio  $\langle W \rangle^* / \langle W \rangle^{\text{lin}}$  and the reduction in computational cost calculated for the optimized protocols are shown as a function of the trap displacement in Fig. 7, respectively. For small trap displacements the work optimized and the error optimized yield similar improvements. For larger displacements, however, the work optimized protocol leads to an increase in the computational cost of the free-energy computation. Similarly, the error optimized protocol reduces the computational cost while leading to an increase in the average work with respect to the linear protocol. In the

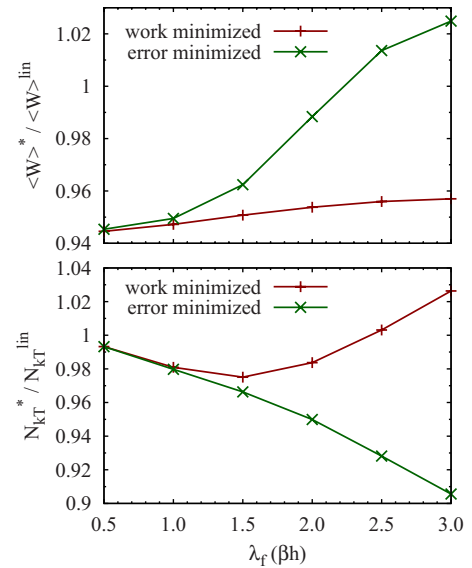


FIG. 7. (Color online) Work ratio  $\langle W \rangle^* / \langle W \rangle^{\text{lin}}$  (top) and reduction in computational cost  $\eta = N_{KT}^* / N_{KT}^{\text{lin}}$  (bottom) as a function of the total displacement  $\lambda_f$  of the V-shaped trap for the minimum work protocol and the minimum error protocol, respectively.



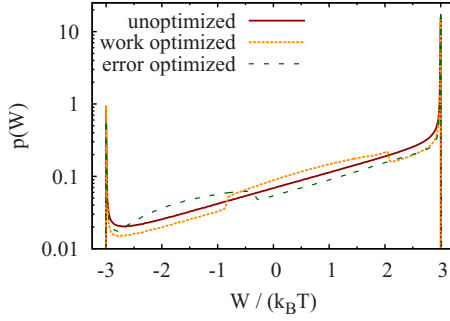


FIG. 8. (Color online) Work distributions obtained for the V-shaped trap for  $\lambda_f = 3\beta h$  using the linear protocol, the minimum work protocol and the minimum error protocol. These work distributions were obtained from  $10^8$  trajectories integrated with a time step of  $\delta t = 0.002\kappa^{-1}$ .

best case studied for this example, the reduction in computational cost is about 10% and a reduction in similar magnitude is observed for the average work.

The work distributions generated using the linear protocol and the two optimum protocols, shown in Fig. 8, differ noticeably. Due to the particular shape of the trap, the work distribution is strictly bound from above and below. The maximum amount of work,  $W_{\max} = h\lambda_f$ , is performed along trajectories for which the particle is on the left of the trap center experiencing a force of  $F = h$  at all times during the transformation. Trajectories for which the particle resides on the right of the trap center, on the other hand, lead to the least possible amount of work,  $W_{\min} = -h\lambda_f$ . At  $W_{\min}$  and  $W_{\max}$  the work distribution has two singularities, caused by the finite fraction of trajectories for which the particle never crosses the trap center during the transformation. Trajectories, along which the trap center is crossed repeatedly lead to intermediate work values,  $-h\lambda_f < W < h\lambda_f$ . The optimum work protocol achieves the work reduction essentially by lowering the statistical weight of the high work peak at  $W_{\max} = h\lambda_f$  and increasing that of the low work peak at  $W_{\min} = -h\lambda_f$ . Interestingly, the optimum work and the optimum error protocol lead to an almost complementary step structure in the intermediate work range, most likely due to the combined effect of the discrete jumps of the control parameter at the start and the end of the switching process. Note, however, that the significance of these steps in the work distribution is exaggerated by the logarithmic scale used on the ordinate of Fig. 12.

The maximum amount of work is carried out if the trap is translated in a sudden jump from  $\lambda_i$  to  $\lambda_f$ . In this case, the work distribution is given by

$$p_{\text{jmp}}(W) = \frac{1}{2}\delta(W - h\lambda_f) + \frac{e^{-\beta h\lambda_f}}{2}\delta(W + h\lambda_f) + \frac{\beta}{4}e^{-\beta(h\lambda_f - W)/2}\theta(W + h\lambda_f)[1 - \theta(W - h\lambda_f)], \quad (39)$$

where  $\delta(x)$  is the Dirac delta function and  $\theta(x)$  is the Heaviside step function. Thus, the work distribution for the sudden

transformation has delta peaks of different magnitude at  $W = h\lambda_f$  and  $W = -h\lambda_f$ , respectively, and varies continuously between these two values. Outside the interval  $[-h\lambda_f, h\lambda_f]$  the work distribution vanishes. For the sudden jump, the average work obtained by integration over the work distribution equals

$$\langle W \rangle^{\text{jmp}} = k\lambda - \frac{1}{\beta}(1 - e^{-\beta h\lambda}). \quad (40)$$

Here, the first term results from particles lifted by  $h\lambda$  during the jump and the second term is a correction caused by a slightly smaller lift for the particles that are on the right of the trap center in the equilibrium distribution of the trap located at  $\lambda_i$ . For trap displacements that are large compared to the width of the equilibrium distribution,  $\lambda \gg 1/\beta k$ , the average work is  $\langle W \rangle^{\text{jmp}} \approx h\lambda - 1/\beta$ . The average work values obtained for the optimum protocols are considerably lower than the average work of the jump protocol. For instance, with respect to the jump protocol, the average work of the optimum protocol is reduced by 40% and 12% for  $\lambda_f = 0.5\beta h$  and  $\lambda_f = 3.0\beta h$ , respectively. From the work distribution of Eq. (39) one can also determine the number of sudden transformations required to obtain an accuracy of about 1  $k_B T$  in the free-energy estimate,

$$N_{kT}^{\text{jmp}} = \langle e^{-2\beta W} \rangle^{\text{jmp}} = \frac{1}{3}e^{-2\beta h\lambda} + \frac{2}{3}e^{\beta h\lambda}, \quad (41)$$

a number which grows rapidly with increasing trap displacement and is considerably larger than the number of trajectories required for the minimum error protocol. For trap displacements of  $\lambda_f = 0.5\beta h$  and  $\lambda_f = 3.0\beta h$ , for instance, the minimum error protocol yields a reduction in  $N_{kT}$  of 8% and 14%, respectively.

### C. Shifted harmonic trap on nonflat landscape

As a further example with a non-Gaussian work distribution we consider a particle in a harmonic trap experiencing an additional external time-independent force. The particle evolves according to the overdamped Langevin equation with potential energy

$$U(x, t) = \frac{k}{2}[x - \lambda(t)]^2 + U_a(x), \quad (42)$$

where the external potential, depicted in Fig. 9, is given by

$$U_a(x) = \varepsilon[1 - (x/\sigma - 1)^2]^2 + \frac{\varepsilon}{2}(x/\sigma - 1). \quad (43)$$

Here,  $k$  is a force constant and  $\varepsilon$  and  $\sigma$  are constants with units of energy and length, respectively. The above potential (see Fig. 9) has minima at  $x \approx 0$  and  $x \approx 2$  and in the course of the transformation the trap is moved from  $\lambda_i = 0$  to  $\lambda_f$  in a time  $\tau$ . This example is chosen to mimic a biomolecule with two stable conformations that is stretched mechanically, for instance using optical tweezers [39]. Due to the external potential  $U_a(x)$  the free-energy difference between the equilibrium states corresponding to the initial and final trap positions takes a nonzero value in contrast to the previous two

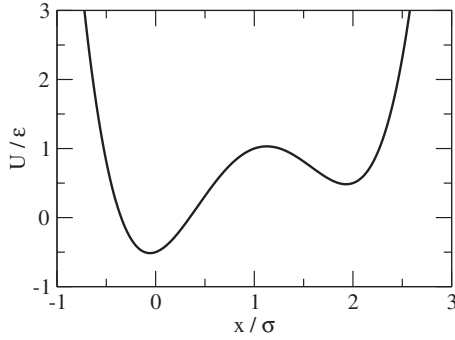


FIG. 9. External potential  $U_a(x)$  acting on the particle as it is translated in the moving harmonic trap.

examples. In the following, we measure energies in units of  $k_B T$ , lengths in units of  $1/\sqrt{\beta k}$ , and times in units of  $\kappa^{-1} = \gamma/k$ .

Minimum work protocols obtained for trajectories of length  $\tau = 1\kappa^{-1}$ , a trap displacement of  $\lambda_f = 2/\sqrt{\beta k}$  and various strengths of the external potential are shown in the top panel of Fig. 10. For each iteration  $2 \times 10^8$  trajectories were generated with a time step of  $\delta t = 0.002\kappa^{-1}$ . Minimum error protocols for the same set of parameters are shown in the bottom panel of Fig. 10. As in the previous examples, discrete steps develop at the beginning and the end of the switching process both for the optimum work protocol and the optimum error protocol. While for small strengths  $\epsilon$  of the external potential the minimum work and the minimum error protocol are very similar, for large  $\epsilon$  the steps of the minimum error protocol are more pronounced.

The reduction in work achieved by the minimum work protocol and the minimum error protocol with respect to the linear protocol is depicted in the top panel of Fig. 11 as a function of the strength  $\epsilon$  of the external potential. As ex-

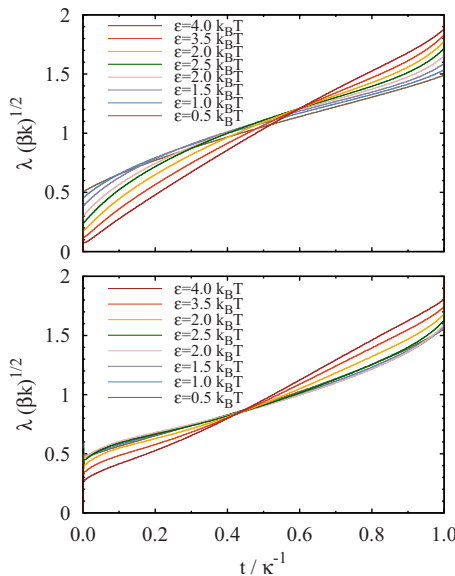


FIG. 10. (Color online) Minimum work protocols (top) and minimum error protocols (bottom) for the harmonic trap shifted on a nonflat energy landscape for various strengths  $\epsilon$  of the external potential. The trajectories length was  $\tau = 1\kappa^{-1}$  and  $\sigma = 1/\sqrt{\beta k}$ .

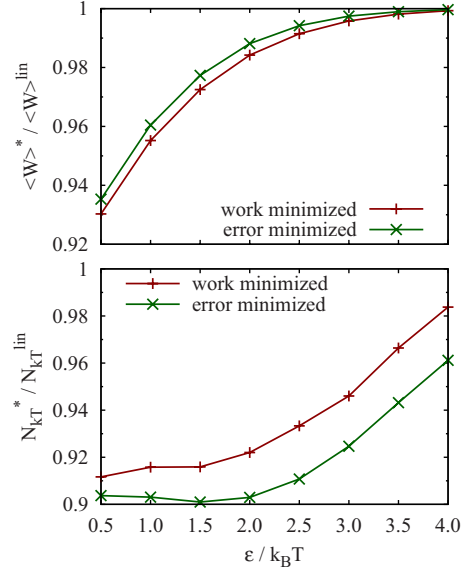


FIG. 11. (Color online) Work ratio  $\langle W \rangle^* / \langle W \rangle^{\text{lin}}$  and reduction in computational cost  $\eta = N_{kT}^* / N_{kT}^{\text{lin}}$  as a function of the strength  $\epsilon$  of the external potential for the minimum work protocol and the minimum error protocol, respectively.

pected, the average work for the minimum work protocol is lower than that of the minimum error protocol, although they differ only slightly. The work reduction is most pronounced for small strengths  $\epsilon$ . A similar dependence on the strength  $\epsilon$  is observed for the reduction in computational cost, shown in the bottom panel of Fig. 11. The reduction in computational cost, reaching up to about 10%, is more pronounced than the reduction in work, which does not exceed 6% in the parameter range of our calculations.

Work distributions obtained for the linear protocol and the optimized protocols are shown in Fig. 12. For each distribution,  $10^8$  trajectories of length  $\tau = 1\kappa^{-1}$  were generated with a time step of  $\delta t = 0.002\kappa^{-1}$ . In this case, the work distributions of the optimum work and optimum error protocols are very similar, but they differ considerably from the work distribution of the linear protocol.

#### D. Stretched polymer

As a higher-dimensional example, we study a polymer that is stretched while it evolves deterministically according

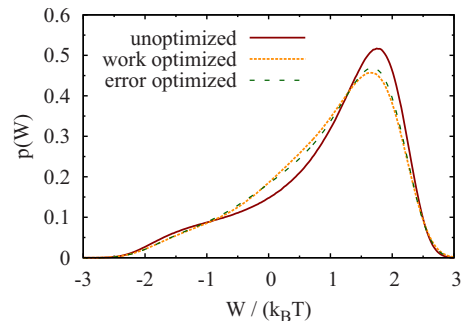


FIG. 12. (Color online) Work distributions obtained using various protocols for the harmonic trap translated on a non-flat energy landscape for an external potential strength of  $\epsilon = 0.5k_B T$ .

to Newton's equations of motion. Our calculations indicate that also in this case discrete jumps of the control parameter at the beginning and at the end of the switching process reduce both the average work as well as the statistical error in the free-energy estimate.

The model polymer consists of a string of  $N$  beads of mass  $m$  with positions  $\mathbf{r}_i$  and momenta  $\mathbf{p}_i$  connected with harmonic springs to their neighbors. The Hamiltonian of the system is given by

$$\mathcal{H} = \sum_{i=1}^N \frac{\mathbf{p}_i^2}{2m} + \sum_{i=1}^{N-1} U_b(r_{ii+1}) + \sum_{i=1}^{N-2} \sum_{j=i+2}^N U_{\text{WCA}}(r_{ij}), \quad (44)$$

where  $r_{ij} = |\mathbf{r}_j - \mathbf{r}_i|$  is the distance between particles  $i$  and  $j$ . The bond potential

$$U_b(r) = \frac{k}{2}(r - R)^2, \quad (45)$$

keeps the distance between subsequent beads close to the equilibrium distance  $R$ . Particles not connected by such a bond interact via the purely repulsive Weeks-Chandler-Anderson potential [40],

$$U_{\text{WCA}}(r) = \begin{cases} 4\epsilon \left[ \left( \frac{\sigma}{r} \right)^{12} - \left( \frac{\sigma}{r} \right)^6 \right] + \epsilon & \text{for } r \leq 2^{1/6}\sigma, \\ 0 & \text{for } r > 2^{1/6}\sigma, \end{cases} \quad (46)$$

where  $\epsilon$  and  $\sigma$  are parameters setting the strength and the interaction range of the particles, respectively. The instantaneous state  $x$  of the system is specified by the positions and momenta of all particles,  $x = \{\mathbf{r}_1, \mathbf{r}_2, \dots, \mathbf{r}_N, \mathbf{p}_1, \mathbf{p}_2, \dots, \mathbf{p}_N\}$ . In the following, we measure lengths in units of  $\sigma$ , energies in units of  $\epsilon$  and times in units of  $(\epsilon/m\sigma^2)^{-1/2}$ .

The polymer is stretched by controlling its end-to-end distance  $r = |\mathbf{r}_N - \mathbf{r}_1|$ , i.e., the distance between the first and last bead in the string. The stretching process is performed as follows. First, an initial configuration is generated using a canonical Monte Carlo simulation at reciprocal temperature  $\beta$  with end-to-end distance fixed at a given initial value  $r_i$ . After assigning momenta from the appropriate Maxwell-Boltzmann distribution, the Newtonian equations of motion are then integrated stepwise with a time step  $\delta t$  using the velocity Verlet algorithm. During the molecular dynamics steps, the first and last beads of the polymer are kept at fixed positions while all other atoms evolve according to the equations of motion. After each step, however, the control parameter, i.e., the end-to-end distance  $r$ , is increased by an amount  $\Delta\lambda$  prescribed by the protocol  $\lambda(t)$ . The change in the control parameter  $r$  is carried out by displacing instantaneously the first and the last bead by  $\Delta\mathbf{r}_1 = -(\Delta\lambda/2)\mathbf{e}$  and  $\Delta\mathbf{r}_N = (\Delta\lambda/2)\mathbf{e}$ , respectively. Here,  $\mathbf{e} = (\mathbf{r}_N - \mathbf{r}_1)/|\mathbf{r}_N - \mathbf{r}_1|$  is the unit vector pointing from bead 1 to bead  $N$ . Using these trajectories, the exponential work average is evaluated with the large time step method [19], which permits an in principle exact free-energy computation even if the individual trajectories are inaccurate due to the finite size of the time step  $\delta t$ .

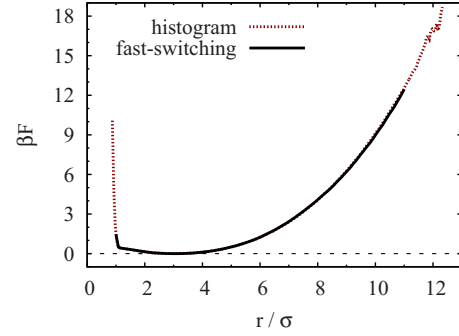


FIG. 13. (Color online) Reversible work  $F(r)$  as a function of the end-to-end distance  $r$  for a polymer with  $N=10$  beads and for parameters  $k=10\epsilon/\sigma^2$  and  $R=\sigma$  computed from a fast-switching simulation (solid line) and a canonical molecular dynamics simulation (dotted line). In the fast-switching simulation  $10^5$  trajectories of length  $\tau=100(\epsilon/m\sigma^2)^{-1/2}$  were integrated and the molecular dynamics simulation consisted of  $10^{11}$  time steps of length  $\delta t = 0.001(\epsilon/m\sigma^2)^{-1/2}$ .

For reference, we have calculated the free energy as a function of the end-to-end distance using a canonical molecular dynamics simulation with an Andersen thermostat [41]. This can be done by computing the distribution  $P(r)$  of the end-to-end distances,

$$P(r) = \langle \delta[r - r(x)] \rangle, \quad (47)$$

where  $r(x)$  denotes the end-to-end distance in state  $x$ . The free energy  $F(r)$ , or, more precisely, the reversible work required to change the end-to-end distance  $r$ , is then given up to an irrelevant constant by

$$F(r) = -k_B T \ln P(r) + 2k_B T \ln r. \quad (48)$$

The last term in the above equation corrects for the number of configurations available at a given end-to-end distance  $r$ , which is proportional to the surface area of a sphere with radius  $r$ . The free energy  $F(r)$  computed in this way for a polymer of  $N=10$  beads at a reciprocal temperature of  $\beta = 1/\epsilon$  is shown in Fig. 13. At small end-to-end distances  $r$  the reversible work  $F(r)$  increases to the direct repulsion of the first and the last bead. At large  $r$ , the increase is caused by the combined energetic effect of the harmonic springs and the entropic contribution due to the smaller number of configurations available to the intermediate beads.

Since the dynamics considered here is deterministic rather than stochastic, we cannot determine the optimum protocol in the way described in Sec. III. Instead, we optimize the protocol in a restricted subspace without using gradients in the optimization procedure. We consider a protocol with instantaneous jumps of arbitrary heights  $\Delta\lambda_i$  and  $\Delta\lambda_f$  at the beginning and the end, respectively. Between the jumps, the control parameter is a linear function of time,  $\lambda(t) = \lambda_i + \Delta\lambda_i + (\lambda_f - \Delta\lambda_f - \lambda_i - \Delta\lambda_i)t/\tau$ . For a particular trajectory length  $\tau$ , the average work and the number of required trajectories are then functions of the two step sizes  $\Delta\lambda_i$  and  $\Delta\lambda_f$ , which completely specify the protocol. Although the requirement of a linear central part may be a strong constraint imposed on the protocol, it is nevertheless interesting to know, whether

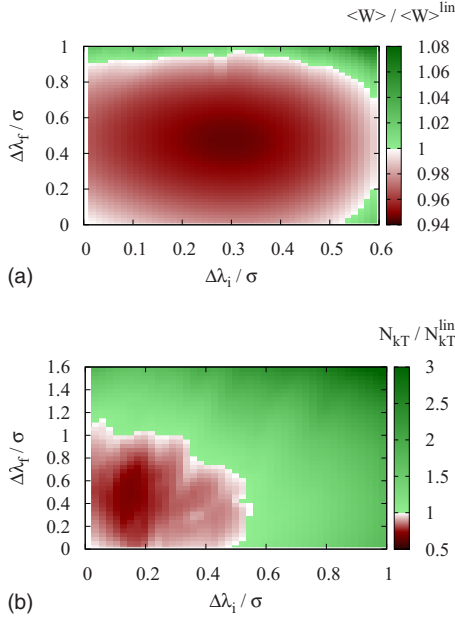


FIG. 14. (Color online) Color coded map of the average work  $\langle W \rangle$  (top) and of the reduction in computational cost  $\eta = N_{kT} / N_{kT}^{\text{lin}}$  (bottom) for the stretched polymer as a function of the jump sizes  $\Delta\lambda_i$  and  $\Delta\lambda_f$  at the beginning and the end of the stretching process, respectively.

discrete steps in the protocol are beneficial in terms of the average work and the statistical error in this restricted protocol space. A more general representation of the protocols, for instance using polynomial functions, can be used to find better approximations to the optimum protocols.

To find the jump sizes of the minimum work protocol, we have determined the average work  $\langle W \rangle$  for  $60 \times 60$  pairs  $\{\Delta\lambda_i, \Delta\lambda_f\}$  of jump sizes. The jump sizes are selected at regular distances from the interval  $[0\sigma, 1\sigma]$ . In each calculation,  $5 \times 10^5$  trajectories of length  $\tau = 3(\epsilon/m\sigma^2)^{-1/2}$  were integrated with a time step of  $\delta t = 0.01(\epsilon/m\sigma^2)^{-1/2}$  while the control parameter was changed from  $\lambda_i = 3\sigma$  to the final  $\lambda_f = 9\sigma$ . This rather large time step can be used, because the Jarzynski equation is evaluated using the larger time step formalism [19]. The corresponding free-energy difference is  $\beta\Delta F = 6.2763 \pm 0.0001$ . [This accurate free-energy estimate was obtained from  $3.2 \times 10^8$  trajectories of length  $\tau = 50(\epsilon/m\sigma^2)^{-1/2}$ .] The average work computed in these simulation is shown in the top panel of Fig. 14 as a color coded map as a function of the two jump sizes  $\Delta\lambda_i$  and  $\Delta\lambda_f$ . The average work has a clear minimum for jump sizes of  $\{0.3\sigma, 0.48\sigma\}$ . For these optimum jump sizes the average work is  $\langle W \rangle = 10.58\epsilon$ , roughly 5% smaller than the average work obtained with the linear protocol.

The size of the jumps in the minimum work protocol depends strongly on the total switching time  $\tau$ . To study this dependence, we have determined the minimum work protocol for different times  $\tau$  using the procedure described in the previous paragraph with  $44 \times 44$  grid points and  $10^5$  trajectories for each pair of jump sizes. Initial and final jump sizes are depicted in Fig. 15 as a function of  $\tau$ . As observed for the pulled harmonic trap, the jumps are most pronounced in the fast-switching regime and become smaller with increasing switching times.

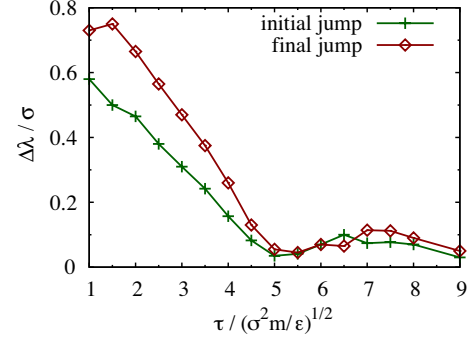


FIG. 15. (Color online) Magnitudes  $\Delta\lambda_i$  and  $\Delta\lambda_f$  of the initial and final jumps of the minimum work protocols as a function of the switching time  $\tau$  for the stretched polymer.

For trajectories of length  $\tau = 3(\epsilon/m\sigma^2)^{-1/2}$ , as used in the work minimization, the calculation of the number of required trajectories  $N_{kT} = \langle \exp(-2\beta W) \rangle$  is difficult for the reasons described in Sec. II. Therefore, we estimate  $N_{kT}$  by calculating the error  $\epsilon^2$  according to Eqs. (5) and (6) from 2000 sets of  $10^4$  trajectories. The reduction in computational cost  $N_{kT} / N_{kT}^{\text{lin}}$  with respect to the linear protocol calculated in this way for a grid of  $44 \times 44$  pairs of jump sizes  $\{\Delta\lambda_i, \Delta\lambda_f\}$  is shown in the bottom panel of Fig. 14. As can be inferred from the figure, a minimum arises near  $\{0.15\sigma, 0.53\sigma\}$ , at which the number of required trajectories is reduced by about 30% compared to the calculation with the linear protocol. Thus, also for the stretched polymer discontinuous jumps at the beginning and the end of the protocol reduce both the average work and the computational effort.

## V. CONCLUSIONS

The Jarzynski equality relating equilibrium free energies to the statistics of work performed on a system by manipulating a control parameter holds for arbitrary switching protocols. The accuracy of free energies extracted from such fast-switching experiments or simulations, however, sensitively depends on the particular protocol according to which the control parameter is driven from its initial to its final value. This freedom can be exploited to design protocols that optimize the free-energy computation. The accuracy of the free-energy estimate is especially affected by the temporal duration of the switching process [8,9,20]. While for slow switching the exponential average of the Jarzynski equality can be accurately computed, large statistical errors make the fast-switching method impractical for large switching rates. The accuracy of the free-energy estimate, however, does not only depend on the rate at which the control parameter is changed, but also in the particular shape of the protocol. As recently shown by Seifert and Schmiedl [15,18], protocols with discrete jumps of the control parameter at the beginning and at the end of the switching process can lead to a considerable reduction in the average work carried out on the system. In this paper we have determined optimum protocols for given duration of the switching process for various example systems. Doing this, we have paid special attention to the question of whether discrete steps in the protocol reduce not

only the average work but also the expected error of the free-energy estimate.

To find the protocols that minimize the average work and the statistical error we have used a numerical steepest descent procedure, in which the values of the control parameter at different times are the variational parameters that are adjusted in the optimization process. In all cases studied in this paper, which include one-dimensional stochastic systems but also a higher dimensional model evolving deterministically, the resulting minimum work and minimum error protocols have discrete steps at the beginning and at the end (but never in between) with magnitudes that strongly depend on the parameters. These steps are particularly pronounced in the fast-switching limit and they disappear for low switching rates. In slow switching limit, where the work distributions become Gaussian, the minimum error protocols and the minimum work protocols become identical. For fast switching, however, the two protocols can differ significantly. In some parameter ranges, the minimum work protocol even leads to an increase in the error compared to the linear protocol without steps. Similarly, under certain conditions, the minimum error protocol can yield an average work larger than that performed with a linear protocol.

In the case of the particle in the moving harmonic trap, the minimum work protocol determined analytically by Schmiedl and Seifert [15] leads to a decrease in the average work of up to 12% compared to a linear protocol without steps. We observed work reductions in similar magnitude for the minimum work protocols determined numerically for the model systems studied in the previous section. Optimizing the protocol with respect to the expected error in the free-energy estimate, on the other hand, can have a much more pronounced effect. As we have demonstrated analytically for

the particle in the harmonic trap, the computational cost required to obtain a certain accuracy in the free-energy estimate for a given total duration of the transformation can be reduced dramatically by incorporating appropriate discrete steps in the protocol.

Indeed, in the fast-switching limit, the computational cost relative to the cost resulting for step-free protocol becomes arbitrarily small. However, such large improvements occur only for parameter ranges for which free-energy calculations using a straightforward application of the Jarzynski equation are impractical even with the optimized protocol. The same conclusion must be drawn from the results of our numerical calculations. Also in these cases, minimum error protocols may yield substantial computational savings in the calculation of free-energy energies. In the parameter ranges (switching time, trap displacement) where the relative improvements are appreciable, however, the statistical errors in the computation of the Jarzynski average are so large even with the optimized protocol that an accurate calculation of free-energy differences is unfeasible. It seems that the optimization of other parameters, such as the temporal length of the switching process, is more likely to yield appreciable improvements of fast-switching free-energy calculations. Whether work biased path sampling techniques [9,42] may offer a way to exploit the potential power of optimized protocols is an open question and will be the subject of future studies in our group.

#### ACKNOWLEDGMENTS

We thank Andy Ballard for a critical reading of the manuscript. This work was supported by the Austrian Science Fund (FWF) under Grant No. P20942-N16 and within the Science College “Computational Materials Science” under Grant No. W004.

- 
- [1] J. Hermans, *J. Phys. Chem.* **95**, 9029 (1991).  
 [2] C. Jarzynski, *Phys. Rev. Lett.* **78**, 2690 (1997).  
 [3] C. Jarzynski, *Phys. Rev. E* **56**, 5018 (1997).  
 [4] E. Schöll-Paschinger and C. Dellago, *J. Chem. Phys.* **125**, 054105 (2006).  
 [5] G. E. Crooks, *J. Stat. Phys.* **90**, 1481 (1998).  
 [6] G. E. Crooks, *Phys. Rev. E* **60**, 2721 (1999).  
 [7] F. Ritort, *J. Phys.: Condens. Matter* **18**, R531 (2006).  
 [8] J. Gore, F. Ritort, and C. Bustamante, *Proc. Natl. Acad. Sci. U.S.A.* **100**, 12564 (2003).  
 [9] H. Oberhofer, C. Dellago, and P. L. Geissler, *J. Phys. Chem. B* **109**, 6902 (2005).  
 [10] C. Jarzynski, *Phys. Rev. E* **73**, 046105 (2006).  
 [11] *Free Energy Calculations. Theory and Applications in Chemistry and Biology*, edited by C. Chipot and A. Pohorille (Springer Verlag, Berlin, 2006).  
 [12] W. Lechner and C. Dellago, *J. Stat. Mech.* 2007, P04001.  
 [13] R. J. Zwanzig, *J. Chem. Phys.* **22**, 1420 (1954).  
 [14] J. G. Kirkwood, *J. Chem. Phys.* **3**, 300 (1935).  
 [15] T. Schmiedl and U. Seifert, *Phys. Rev. Lett.* **98**, 108301 (2007).  
 [16] M. de Koning, *J. Chem. Phys.* **122**, 104106 (2005).  
 [17] H. Then and A. Engel, *Phys. Rev. E* **77**, 041105 (2008).  
 [18] A. Gomez-Marin, T. Schmiedl, and U. Seifert, *J. Chem. Phys.* **129**, 024114 (2008).  
 [19] W. Lechner, H. Oberhofer, C. Dellago, and P. L. Geissler, *J. Chem. Phys.* **124**, 044113 (2006).  
 [20] G. Hummer, *J. Chem. Phys.* **114**, 7330 (2001).  
 [21] M. R. Shirts, E. Bair, G. Hooker, and V. S. Pande, *Phys. Rev. Lett.* **91**, 140601 (2003).  
 [22] S. X. Sun, *J. Chem. Phys.* **118**, 5769 (2003).  
 [23] E. Atilgan and S. X. Sun, *J. Chem. Phys.* **121**, 10392 (2004).  
 [24] F. M. Ytreberg and D. M. Zuckerman, *J. Chem. Phys.* **120**, 10876 (2004).  
 [25] F. M. Ytreberg and D. M. Zuckerman, *J. Comput. Chem.* **25**, 1749 (2004).  
 [26] D. Wu and D. A. Kofke, *J. Chem. Phys.* **122**, 204104 (2005).  
 [27] D. A. Kofke, *Mol. Phys.* **104**, 3701 (2006).  
 [28] S. Vaikuntanathan and C. Jarzynski, *Phys. Rev. Lett.* **100**, 190601 (2008).  
 [29] D. D. L. Minh, *J. Chem. Phys.* **130**, 204102 (2009).  
 [30] A. M. Hahn and H. Then, *Phys. Rev. E* **79**, 011113 (2009).  
 [31] D. M. Zuckerman and T. B. Woolf, *Phys. Rev. Lett.* **89**, 180602 (2002).

- [32] G. Adjanor, M. Athenes, and F. Calvo, *Eur. Phys. J. B* **53**, 47 (2006).
- [33] G. E. Lindberg, T. C. Berkelebach, and F. Wang, *J. Chem. Phys.* **130**, 174705 (2009).
- [34] W. H. Press, S. A. Teukolsky, W. T. Vetterling, and B. P. Vetterling, *Numerical Recipes* (Cambridge University Press, Cambridge, England, 1988).
- [35] M. P. Allen and D. J. Tildesley, *Computer Simulation of Liquids* (Clarendon, Oxford, 1987).
- [36] C. Dellago, P. G. Bolhuis, F. S. Csajka, and D. Chandler, *J. Chem. Phys.* **108**, 1964 (1998).
- [37] O. Mazonka and C. Jarzynski, e-print arXiv:cond-mat/9912121.
- [38] A. Saha, S. Lahiri, and A. M. Jayannavar, *Phys. Rev. E* **80**, 011117 (2009).
- [39] H. Oberhofer, C. Dellago, and S. Boresch, *Phys. Rev. E* **75**, 061106 (2007).
- [40] J. D. Weeks, D. Chandler, and H. C. Andersen, *J. Chem. Phys.* **54**, 5237 (1971).
- [41] H. C. Andersen, *J. Chem. Phys.* **72**, 2384 (1980).
- [42] H. Oberhofer and C. Dellago, *Comput. Phys. Commun.* **179**, 41 (2008).